Strength and Adaptation of Stereolithography-Fabricated Zirconia Dental Crowns: An In Vitro Study

Rong Li, PhD

Yong Wang, MS

Center of Digital Dentistry, Department of Prosthodontics, Peking University School and Hospital of Stomatology, Beijing, China

Menglong Hu, PhD

Yungan Wang, PhD

Porimy 3D Printing Technology, Kunshan, China

Yongxiang Xv, PhD

Department of Dental Materials, Peking University School and Hospital of Stomatology, Beijing, China

Yushu Liu, DDS

The Second Clinical Division, Peking University School and Hospital of Stomatology, Beijing, China

Yuchun Sun, PhD

Center of Digital Dentistry, Department of Prosthodontics, Peking University School and Hospital of Stomatology, Beijing, China

Purpose: To evaluate the physical and mechanical properties of zirconia ceramic manufactured with stereolithography and to quantitatively analyze the internal and marginal adaptation of the zirconia ceramic dental crowns. ***Materials and Methods:*** A resin-based zirconia suspension with a solid content of 45 vol% was prepared. Zirconia dental crowns (n = 5) for the maxillary right first molar were designed and manufactured. Physical and mechanical properties—including density, sintering shrinkage, flexural strength, Weibull parameters, phase composition, and microstructure—of the stereolithography-manufactured zirconia crowns were evaluated. A three-dimensional subtractive analysis technique was used to evaluate the internal and marginal adaptation. ***Results:*** The stereolithography-manufactured zirconia (n = 22) achieved a flexural strength of 812 ± 128 MPa and a Weibull modulus of 7.44. Quantitative analysis of the fabricated zirconia crowns showed a cement space of 63.40 ± 6.54 μm in the occlusal area, 135.08 ± 10.55 μm in the axial area, and 169.58 ± 18.13 μm in the marginal area. ***Conclusion:*** Within the limits of this study, the strength of the stereolithography-manufactured zirconia was adequate for fabricating dental crowns. However, internal and marginal adaptation are not yet ideal for clinical application. *Int J Prosthodont 2019;32:439–443. doi: 10.11607/ijp.6262*

Compared to metal and resin, ceramic is the preferred material for fabricating dental restorations, owing to its chemical stability, biocompatibility, and tooth-like color.[1,2] In the past decades, the advent and development of subtractive computer-aided design/computer-assisted manufacturing (CAD/CAM) technology have enabled all-ceramic restorations to be reliable, with accurate dimensions and reduced manufacturing time.[2,3] Toughened by phase transformation, yttria-stabilized zirconia ceramic is gaining popularity in clinical practice and has become the first choice for posterior dental restorations. However, the subtractive method requires milling tools, and the costs of the final machining process account for 70% to 80% of the total cost.[4] Besides, introduction of invisible microscopic cracks from the milling process could undermine the strength of the restoration,[5] resulting in a concentration of stress that could potentially lead to clinical failure. To overcome these issues, recent research has explored the feasibility of additive manufacturing of zirconia in

Correspondence to:
Prof Yuchun Sun
Peking University School and Hospital of Stomatology
No. 22, Zhongguancun South Street
Haidian District, Beijing, China
Email: polarshining@163.com

Submitted November 23, 2018; accepted April 25, 2019.

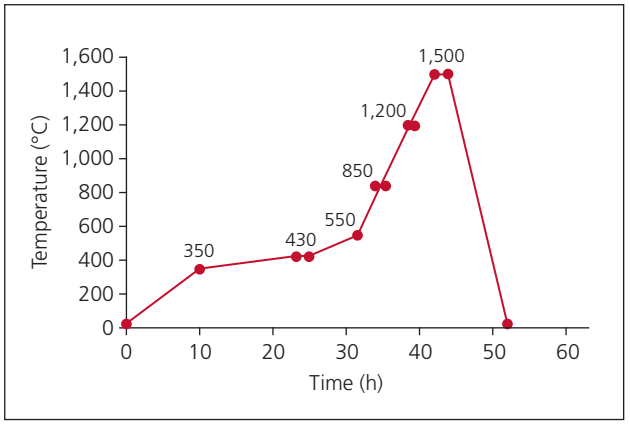

Fig 1 Heat treatment schedule. 350°C to 550°C = de-binding stage (organic binder is burned out and a slow heating rate is applied to avoid crack formation); 550°C to 1,500°C = sintering stage (zirconia particles crystallize and densify).

Table 1 Specifications of the Stereolithography Manufacturing

Items	Parameters
Layer thickness	25 μm
Beam diameter of the scanner	25 μm
Laser scan speed	750 mm/s (scan twice for every layer)
Laser power	0.308 w

dentistry.[6,7] Contrary to the subtractive method, additive manufacturing shapes a three-dimensional (3D) solid model on a layer-by-layer basis. So far, ceramic and ceramic-based composites are limited in additive manufacturing processes,[8] lagging behind metal and polymer.

Additive manufacturing methods for zirconia include selective laser sintering/melting (SLS/SLM), 3D printing (3DP), direct inkjet printing (DIP), and lithography-based additive manufacturing. Lithography-based additive manufacturing, including stereolithography (SLA) and digital light processing (DLP), shapes the green body on a layer-by-layer basis by selectively curing a suspension with ceramic particles in photosensitive resin using a laser scanner or a digital micromirror device, which is then followed by heat treatment to achieve a dense ceramic part.[9] Studies on its dental application are limited, and quantitative analysis of the adaptation of the sintered crowns has not been reported yet.

The purpose of this study was to evaluate the physical and mechanical properties of zirconia ceramic manufactured via SLA and to quantitatively analyze the internal and marginal adaptation of the fabricated dental crowns. The hypothesis was that SLA can be applied to produce dental crowns with reliable mechanical strength and adequate adaptation.

MATERIALS AND METHODS

Specimen Model Design

Cuboid (5 × 2.5 × 30 mμ) and disc (diameter 12.5 mm, thickness 2.5 mm) models for characterization of physical and mechanical properties were designed using Imageware and saved in standard tessellation language (STL) file format. The full crown restoration for the right maxillary first molar was designed in the same way as a previous publication.[10] The geometric dimensions of the crown model were scaled up accordingly in order to compensate for shrinkage occurring during sintering.

Fabrication of Specimens

A resin-based zirconia suspension with a solid content of 45 vol% and a top-down projected SLA-printer (CSL 150, Porimy) were applied to print specimens. Specifications of the SLA manufacturing are shown in Table 1. After printing, the green specimens were ultrasonically cleaned and heat treated in a furnace (KSL-1700X, Kejing Materials). The heat treatment profile is depicted in Fig 1 and can be broadly divided into two stages: *(1)* a de-binding stage to burn out the organic composition and *(2)* a sintering step for grain growth, improving its density.

Characterization of Fabricated Specimens

The densities of three sintered specimens were measured using a densitometer (MH-300A, MatsuHaku). A vernier caliper (accuracy 0.01 mm) was used to measure the dimensions of cuboid specimens (n = 28) both in the green and sintered stages to determine linear shrinkage. Flexural strength was determined using a universal testing machine (3367, Instron). A progressive load was applied at a speed of 1 mm/minute. Weibull distribution analysis was performed based on flexural strength data (n = 22) to assess structural reliability, yielding two parameters: the Weibull characteristic strength (σ_0) and the Weibull modulus (m). A high Weibull modulus indicates a high degree of homogeneity and smaller variations in flexural strength. Crystallographic phase analysis was performed using an x-ray diffractometer (XRD, D8 Advance, Bruker). The test was performed in a 10-degree to 90-degree diffraction angle range and at a step interval of 1.25 seconds and a step size of 0.02 degrees. Scanning electron microscopy (SEM) (JSM-7500F, JEOL) was applied to analyze microstructure.

The 3D subtractive analysis technique was used to evaluate internal and marginal adaptation.[11] The preparation and adjacent resin teeth were seated on a specially designed fixed base (Figs 2a and 2b). The intaglio surface of each crown (n = 5) was lightly coated with a layer of silicone oil, which was further blown with high-pressure air to achieve a thin and uniform distribution. The crown was then filled with light-body

polyvinylsiloxane (PVS) (betasil Vario Light, Müller-Omicron) and seated onto the preparation for 5 minutes. After complete polymerization, the crown was carefully removed, leaving a PVS film on the preparation. The thickness of the PVS film was used to represent the thickness of the cement space. Digital models were obtained using an intraoral scanner (CEREC Omnicam, Dentsply Sirona), including a digital scan of the crown preparation and that of the crown preparation with a PVS film over it. Preparation and PVS scans were superimposed using the best-fit algorithm, and a 3D deviation analysis was performed using Geomagic Studio 2012 (Raindrop). Three areas were selected for analysis: the margin (Fig 2f), the axial wall (Fig 2g), and the occlusal surface (Fig 2h).

Statistical Analyses

Statistical analyses were performed using SPSS (SPSS Statistics 19, IBM). Normality of distribution of data was verified using the Shapiro-Wilk test (α = .05). The calculated cement space and the corresponding set value were compared using one-sample *t* test.

RESULTS

Density was measured at 5.83 g/cm³. Fabricated specimens displayed anisotropic shrinkage. The shrink rate was 18.1% in length (x axial), 20% in width (y axial), and 24.3% in height (z axial). Greater shrinkage was determined in height than in length or width. Flexural strength of the sintered component was 812 ± 128 MPa. The Weibull characteristic strength was 866.7 MPa (95% confidence interval [CI] 530.1 to 1,415.2 MPa), and the Weibull modulus was 7.44 (95% CI 6.90 to 7.99).

XRD phase analysis showed a standard pattern for sintered Y-TZP, indicating that the crystalline phase detected on the surface of the specimen was tetragonal zirconia (Fig 3b). SEM micrographs of sintered specimens presented a homogenous microstructure. No layer-by-layer trace or delamination were detected from the lateral surface (Fig 2i). The fracture ends of a flexural strength test specimen showed pores ranging from submicron to several microns (Fig 2j).

Fabricated crowns could be successfully seated on the preparation (Figs 2c and 2d). No adjustments were applied. Quantitative analysis results are presented in Table 2. Results revealed statistically significant differences between the calculated cement space and the set value.

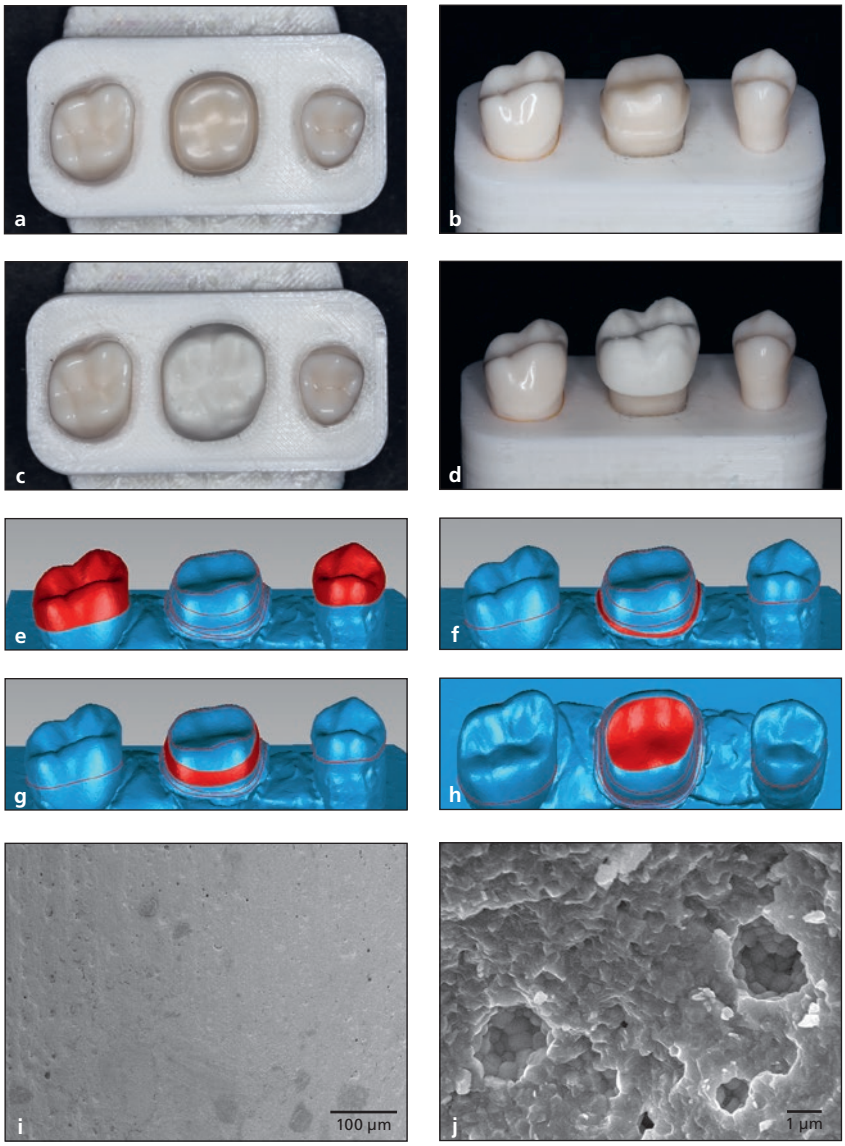

Fig 2 *(a)* Occlusal and *(b)* palatal views of the preparation and adjacent resin teeth seated on a specially designed fixed base. *(c)* Occlusal and *(d)* palatal views of the fabricated crowns seated on the preparation. Three-dimensional analysis of the cement space: *(e)* Area chosen for superimposing two scans (red), *(f)* margin area, *(g)* axial wall area, and *(h)* occlusal surface. SEM of sintered specimens: *(i)* lateral surface (×200), *(j)* fracture ends of a flexural strength test specimen (×10,000).

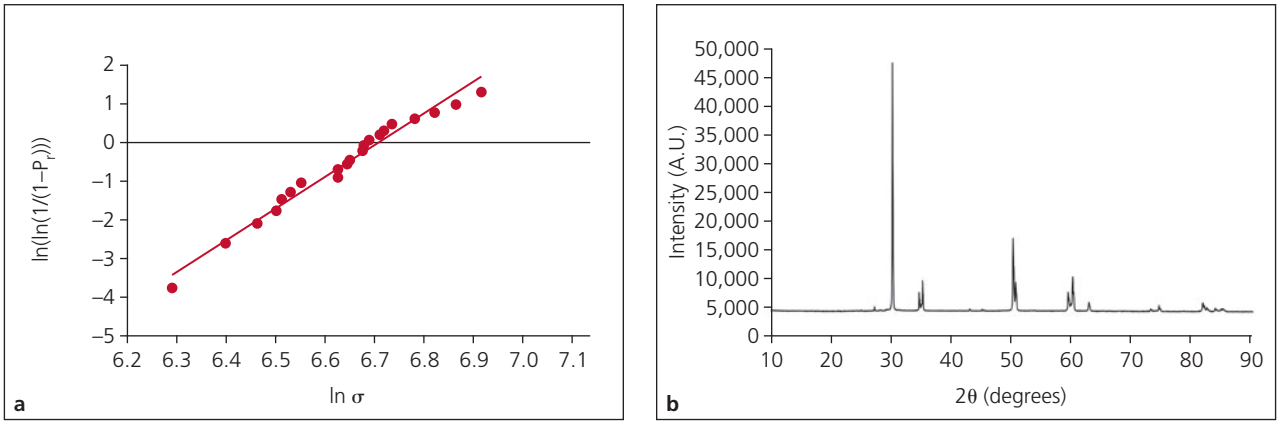

Fig 3 *(a)* Weibull plot of sintered zirconia specimens (n = 22) manufactured with stereolithography. *(b)* X-ray diffraction on the specimen surface.

Table 2 Three-Dimensional Analysis of the Cement Space (μm)

Area	Mean (SD)	Set value	Difference (mean set value)	*P* value
OC	63.4 (6.54)	80	−16.6	.064
AX	135.08 (10.55)	80	55.08	.000
MA	169.58 (18.13)	30	139.58	.000

One-sample *t* test (n = 5). OC = occlusal surface; AX = axial wall; MA = margin.

DISCUSSION

In zirconia SLA technology, the resin serves as a binder to enable shaping of the green specimen and pyrolyzes during the subsequent heat treatment, known as burn-out. Gaseous products pass through the mesh of ceramic particles. In the following sintering stage, zirconia particles crystallize and the specimen is further densified by crystal growth. In order to achieve structural integrity and high strength, the solid content of the suspension, light-curing strategy, and de-binding rates must be carefully controlled to avoid pores, delamination, and cracks. In this study, a flexural strength of 812 ± 128 MPa and a Weibull modulus of 7.44 were achieved, which is adequate for fabricating dental crowns (ISO 6872). Reliable mechanical strength in this study was achieved by adopting a 45-vol% zirconia suspension, small-layer thickness, adequate laser intensity, and longer exposure time. In addition, a slow heating rate was applied.

Internal and marginal adaptation of a restoration are paramount for clinical success. Ideal adaptation helps to keep the abutment and periodontal tissue in a healthy state and achieve high fracture resistance of the restoration. Many researchers and clinicians believe that the value of 120 μm, suggested by McLean and von Fraunhofer,[12] is the most suitable limit for clinical use.[13] Quantitative analysis showed a cement space of 63.40 ± 6.54 μm in the occlusal area, 135.08 ± 10.55 μm in the axial area, and 169.58 ± 18.13 μm in the marginal area in this study, which was not ideal. This can be attributed to light scattering and anisotropic sintering shrinkage. SLA for pure resin is considered to be one of the most accurate additive manufacturing technologies, and its high surface quality makes it suitable for producing castable patterns of dental restorations and surgical templates.[14,15] However, SLA for zirconia is not exactly the same case. When light travels through a suspension, it scatters at the resin-particle interface owing to different refractive indexes.[16] Mitteramskogler et al found that light scattering within ceramic-filled slurry causes a certain amount of widening of dimensions in the final geometry and that this overgrowth is sensitive to both overall exposure area and exposure time.[9] Moreover, shrinkage during heat treatment has a greater influence on manufacturing accuracy and enlargement of dimension when shaping the crown is used to compensate for the shrinkage. In the present study, enlargement parameters for the dental crowns were based on the measured anisotropic shrinkage rate of cuboid specimens. The difference in geometry between crown and cuboid specimens may result in different shrinkage and therefore poor adaptation. To achieve an ideal adaptation, errors induced by light scattering and sintering shrinkage need to be further investigated and controlled.

CONCLUSIONS

Within the limits of this study, the strength of the SLA-manufactured zirconia was adequate to fabricate dental crowns. However, the internal and marginal adaptation were not ideal for clinical application.

ACKNOWLEDGMENTS

This work was supported by the National Key R&D Program of China [grant number 2018YFB1106900], the National Natural Science Foundation of China [grant number 51475004], and the Capital's Funds for Health Improvement and Research [grant number 2018-2-4103]. The authors report no conflicts of interest.

REFERENCES

1. Stawarczyk B, Keul C, Eichberger M, Figge D, Edelhoff D, Lümkemann N. Three generations of zirconia: From veneered to monolithic. Part I. Quintessence Int 2017;48:369–380.
2. Zhang Y, Lawn BR. Novel zirconia materials in dentistry. J Dent Res 2018;97:140–147.
3. Dehurtevent M, Robberecht L, Hornez JC, Thuault A, Deveaux E, Béhin P. Stereolithography: A new method for processing dental ceramics by additive computer-aided manufacturing. Dent Mater 2017;33:477–485.
4. Klocke F. Modern approaches for the production of ceramic components. J Eur Ceram Soc 1997;17:457–465.
5. Wang H, Aboushelib MN, Feilzer AJ. Strength influencing variables on CAD/CAM zirconia frameworks. Dent Mater 2008;24:633–638.
6. Osman RB, van der Veen AJ, Huiberts D, Wismeijer D, Alharbi N. 3D-printing zirconia implants; a dream or a reality? An in-vitro study evaluating the dimensional accuracy, surface topography and mechanical properties of printed zirconia implant and discs. J Mech Behav Biomed Mater 2017;75:521–528.
7. Lian Q, Sui W, Wu X, Yang F, Yang S. Additive manufacturing of ZrO2 ceramic dental bridges by stereolithography. Rapid Prototyping J 2018;24:114–119.
8. Song X, Chen Y, Lee TW, Wu S, Cheng L. Ceramic fabrication using Mask-Image-Projection-based stereolithography integrated with tape-casting. J Manufacturing Processes 2015;20:456–464.
9. Mitteramskogler G, Gmeiner R, Felzmann R, et al. Light curing strategies for lithography-based additive manufacturing of customized ceramics. Additive Manufacturing 2014;1–4:110–118.
10. Liu Y, Ye H, Wang Y, Zhao Y, Sun Y, Zhou Y. Three-dimensional analysis of internal adaptations of crowns cast from resin patterns fabricated using computer-aided design/computer-assisted manufacturing technologies. Int J Prosthodont 2018;31:386–393.
11. Zimmermann M, Valcanaia A, Neiva G, Mehl A, Fasbinder D. Digital evaluation of the fit of zirconia-reinforced lithium silicate crowns with a new three-dimensional approach. Quintessence Int 2018;49:9–15.
12. McLean JW, von Fraunhofer JA. The estimation of cement film thickness by an in vivo technique. Br Dent J 1971;131:107–111.
13. Kim DY, Kim JH, Kim HY, Kim WC. Comparison and evaluation of marginal and internal gaps in cobalt-chromium alloy copings fabricated using subtractive and additive manufacturing. J Prosthodont Res 2018;62:56–64.
14. Cassetta M, Giansanti M, Di Mambro A, Calasso S, Barbato E. Accuracy of two stereolithographic surgical templates: A retrospective study. Clin Implant Dent Relat Res 2013;15:448–459.
15. Kim DY, Jeon JH, Kim JH, Kim HY, Kim WC. Reproducibility of different arrangement of resin copings by dental microstereolithography: Evaluating the marginal discrepancy of resin copings. J Prosthet Dent 2017;117:260–265.
16. Griffith ML, Halloran JW. Scattering of ultraviolet radiation in turbid suspensions. J Appl Phys 1997;81:2538–2546.

Literature Abstract

Influence of Margin Location and Luting Material on the Amount of Undetected Cement Excess on CAD/CAM Implant Abutments and Cement-Retained Zirconia Crowns: An In-Vitro Study.

The flexibility in designing the submucosal part of a computer-aided design/computer-assisted manufacturing (CAD/CAM) customized implant abutment and the individual positioning of its shoulder line have been suggested to reduce the risk of leaving undetected cement residue, thus preventing adverse effects on peri-implant tissues. A high correlation between excess cement left in the soft tissues and the occurrence of increased biofilm accumulation with sulcular bleeding and/or suppuration has been reported. This in turn may cause peri-implant inflammation and peri-implant marginal bone loss. The aim of this study was to assess the frequency of cement remnants after the luting of zirconia crowns on CAD/CAM custom molar abutments with different margin levels and to evaluate the impact of the luting material. A total of 20 titanium molar CAD/CAM implant abutments (BEGO Medical) with internal taper connection/internal hex anti-rotation protection and a convex emergence profile with different margin positions (0, 1, 2, and 3 mm below the mucosa) were virtually designed (Implant Studio, 3Shape) and manufactured. A master cast was scanned and duplicated by a three-dimensional printer, and individual gingival masks were produced to simulate peri-implant soft tissues. Twenty corresponding zirconia crowns were designed (Cerec 3D, Dentsply Sirona), produced, and cemented to the abutments with two different luting materials; a zinc oxide non-eugenol cement (Temp Bond NE) or a methacrylate cement (PANAVIA V5). To ensure retrievability of the crown/abutment connection, occlusal openings providing access to the abutment screws were designed. Excess cement was thoroughly removed, and the crown/abutment units were unscrewed to evaluate the occurrence of cement residue. All the quadrants of each specimen were evaluated for calculation of the ratio between the cement remnant area and the total specimen area using Adobe Photoshop. Spearman analysis was performed to detect correlations between different variables. A two-sided *t* test, analysis of variance (ANOVA), Mann-Whitney test, and Kruskal-Wallis test were applied to detect differences between the groups. Cement remnants were found in every depth of the crown abutment complex and in almost every area investigated. The amount of cement residue increased as the crown-abutment margin was located more submucosally. Lingual areas were more prone to cement remnants than other surface areas ($P = .0291$). Excess cement was not only found at the margins of the crown-abutment complex, but also underneath (basal) the abutment itself, where cleaning was impossible. No statistical difference for the effect of zinc oxide non-eugenol compared to methacrylate cement on the frequency of excess material at the lateral abutment surfaces could be demonstrated in vitro. The proportion of basal abutment aspects covered with cement residue was, however, significantly smaller in PANAVIA V5 samples, with an average of 4.9% ± 3.7% compared to the Temp Bond samples average of 8.6% ± 5.5%. Given the results obtained in the present investigation, the margin of CAD/CAM molar abutments should be located as coronally as possible to minimize the amount of cement remnants. If an epigingival or supragingival margin location is not feasible due to esthetic concerns, it cannot be recommended to place the margin of molar CAD/CAM abutments deeper than 1.5 mm in the proximal and oral regions.

Gehrke P, Bleuel K, Fischer C, Sader R. *BMC Oral Health* 2019;19:111. **References:** 48. **Reprints:** Peter Gehrke, dr-gehrke@prof-dhom.de
—Terry Walton, Australia